Available online at www.sciencedirect.com
SCIENCE DIRECT
Polymer 46 (2005) 12493–12502
polymer
www.elsevier.com/locate/polymer

Nanostructure and crystallisation kinetics of poly(ethylene oxide)/poly (4-vinylphenol-*co*-2-hydroxyethyl methacrylate) blends

Robson Pacheco Pereira, Ana Maria Rocco *

Grupo de Materiais Condutores e Energia, Instituto de Quimica, Universidade Federal do Rio de Janeiro, Cidade Universitária, CT, Bloco A, Rio de Janeiro, RJ, 21945-970, Brasil

Received 16 June 2005; received in revised form 8 August 2005; accepted 31 August 2005
Available online 14 November 2005

Abstract

Blends of poly(ethylene oxide) (PEO) and poly(4-vinylphenol-*co*-2-hydroxyethyl methacrylate) (PVPh-HEM) were studied by means of synchrotron small and wide angle X-ray scattering (SAXS and WAXS, respectively) and by differential scanning calorimetry (DSC). The DSC measurements were used in the determination of the Flory–Huggins interaction parameter and also to study the isothermal and non-isothermal crystallisation kinetics of the PEO/PVPh-HEM blend. The interaction parameter, χ_{12}, was found to be negative (between -0.5 and -2.5, approximately) and presented a significant dependence on the blend composition, which is expected for a system with specific interactions such as hydrogen bonding. From the kinetic studies with Kissinger, Friedman and Avrami models, it was shown that crystallisation of PEO chains is slower in the blend than in the pure polymer, despite the decrease in the energy barrier to the crystallisation with the increase in PVPh-HEM concentration.

From the SAXS and WAXS profiles, the nanostructure of the blend was elucidated, exhibiting the formation of PEO lamellae even in the blends containing high concentrations of PVPh-HEM, which are non-crystalline (as observed by the WAXS profiles). The thickness of the PEO lamellae (R_c, approximately 8 nm) remains almost unchanged with the blend composition, while the crystalline peaks, observed at 19.78 and 23.98°, vanish, and the WAXS profile exhibits only a non-crystalline halo. For the non-crystalline blends with high concentrations of PVPh-HEM, PEO chains keep their crystalline structural memory.

Keywords: Nanostructure; SAXS; Interaction parameter

1. Introduction

Poly(ethylene oxide) (PEO) possesses a relatively simple structure and is capable of packing into crystals, serving as an model polymer for a wide variety of studies and, hence, it has been extensively studied [1]. One of its applications is as host in polymer solid electrolytes (PSE), which are materials of great technological interest because of their applications in solid-state batteries [2], capacitors [3] and electrochromic devices [4]. PSE are characterised by an interesting conductivity behaviour that is highly dependent on the local structure and is influenced by crystallisation and ionic association. PEO is among the first [1] and most studied polymers in PSE, due to the fact that it easily dissolves alkali metal salts. However, it is a semi-crystalline polymer and presents ionic conduction appreciable only above 65 °C [5]. At temperatures below 65 °C, PEO-salt electrolytes consist of mixtures of spherulite crystalline phases separated by non-crystalline solutions of salt in PEO and ion conduction takes place primarily in the non-crystalline regions [6]. However, Andreev and Bruce [7] suggested that some degree of organization in the non-crystalline phase is required for achieving higher conductivities, specifically the helical conformation of PEO.

The strong dependence of the properties on the solid structure can be verified in PSE based on polymer blends of PEO, as shown previously by Rocco and co-workers [8,9]. In these works, the authors show the relation between specific interactions, lithium complexation and chain mobility. As a consequence of these properties, the dependence of the conductivity on the structure is established.

In order to characterise more deeply the semi-crystalline nanostructure of polymer blends, some authors have used small angle X-ray scattering (SAXS) and other related techniques

* Corresponding author. Fax: +55 21 2562 7559.
E-mail address: amrocco@iq.ufrj.br (A.M. Rocco).

0032-3861/$ - see front matter © 2006 Elsevier Ltd. All rights reserved.
doi:10.1016/j.polymer.2005.08.100

(e.g. small angle neutron scattering, SANS), coupled to calorimetric techniques such as differential scanning calorimetry (DSC) and microscopic analysis to do so [10,11].

Crystallisation in polymer blends containing one semi-crystalline and one non-crystalline component is be greatly affected by both miscibility and phase behaviour of the system. The crystallisation kinetics of PEO blends has been studied by DSC [12], SAXS [13,14] and other techniques. This allows a structural and thermal characterisation of PEO blends and the proposal of physical models used to explain the observed properties.

In the present work, Flory–Huggins interaction parameter is determined for isothermally crystallised high molecular mass PEO/poly(4-vinyiphenol-*co*-2-hydroxyethyl methacrylate) (PVPh-HEM) blends [15], and the crystallisation kinetics is also studied, using non-isothermal DSC measurements. Syncrotron SAXS/WAXS measurements were performed in order to obtain nanostructural data on the PEO/PVPh-HEM blends and their crystallisation.

2. Experimental

2.1. Samples preparation

PEO (Aldrich Chem Company, 4×10^6 g mol^{-1}) and PVPh-HEM (Aldrich Chem Company, 1.96×10^6 g mol^{-1}), with ratios from 100/0, to 0/100 wt% were dissolved in methanol (Merck, PA) and the solution was stirred for 8 h. Films were prepared by casting from these solutions on glass plates and dried until constant weight in a desiccator under vacuum.

2.2. Determination of the equilibrium melting temperature

The isothermal crystallisation was performed on a differential scanning calorimeter (DSC, TA Instruments model 2910) based on the Hoffman–Weeks method [16]. The isothermal crystallisation experiment was carried out with the following procedure: samples were heated to 100 °C, kept at this temperature for 5 min, rapidly cooled (cooling rate $>$ 40 °C min^{-1}) to the desired crystallisation temperature (T_c) and maintained at this temperature for 20 min. After the isothermal crystallisation was completed, the samples were cooled to -60 °C and heated to 100 °C at a rate of 10 °C min^{-1} for the measurement of the melting temperature, T_m.

2.3. Crystallisation kinetics

2.3.1. Isothermal kinetics measurement

The non-isothermal crystallization experiments were performed by heating the samples at 100 °C for 5 min and than cooling to -30 °C at cooling rates of 1, 2, 4, 6, 8 and 9 °C min^{-1}. The kinetic models were applied to these DSC data.

One of the first contributions to the kinetic studies of solids was the work of Melvin Avrami [17], which developed a simple, but efficient method to describe crystallisation processes under isothermal conditions:

$$1-\alpha = \exp(-kt^n) \tag{1}$$

where α is the crystallised fraction (the conversion degree), k is the kinetic constant of the process, n is the Avrami exponent and t time. In order to study the experimental data, the log form is utilised:

$$\log(\ln(1-\alpha)) = \log k - n\log t \tag{2}$$

The Avrami analysis allows the identification of kinetic parameters such as the Avrami exponent and the half-life crystallisation time ($t_{1/2}$). The isothermal conditions, however, do not hold for all experiments, and different kinetic models were developed to understand non-isothermal crystallisation processes.

2.4. Non-isothermal kinetics measurement

Among the non-isothermal methods, those proposed by Kissinger [18] and Friedman [19] are widely used in the crystallisation kinetic studies of polymeric materials. The Kissinger method assumes that the observed crystallisation peak (in a thermal scan) is dependent on the scan rate and at the peak, the reaction reaches its maximum velocity. The analytical form for the Kissinger equation is:

$$\frac{\partial\left[\ln\left(\frac{\theta}{T_p^2}\right)\right]}{\partial\left(\frac{1}{T_p}\right)} = -\frac{E_a}{RT} \tag{3}$$

where θ is the scan rate, T_p is the peak temperature observed in the thermal analysis curve, E_a is the activation energy and R the gas constant.

The Kissinger method is often called a peak evolution method and is not limited to the kinetic function of the transformation under study. The Friedman approach, however, consists in an isoconversional method, where the activation energy is determined at different scan rates with temperature values for each certain conversion degree (e.g. $\alpha=50\%$). Since the kinetic equation for a given process may be written as $d\alpha/dt = k(T)f(\alpha)$, where $k(T)$ is the Arrhenius constant, α is the conversion degree and $f(\alpha)$ the function describing the reaction mechanism. When utilising differential scanning calorimetry data, the conversion degree may be defined as $\alpha_i = H_i/Q$, where H_i is the amount of heat involved in a reaction at a conversion degree α_i at the time i and Q is the total amount of heat involved in the overall reaction. The relation above described, in the logarithm form, is:

$$\ln\left(\frac{dH}{dt}\right)_\alpha = \ln(QA_\alpha g(\alpha)) - \frac{E_\alpha}{RT_\alpha} \tag{4}$$

where A_α, E_α, $(dH/dt)_\alpha$ and T_α are, respectively, the pre-exponential factor, activation energy, heat flux and temperature at a certain conversion degree α. This is the equation upon which Friedman based its isoconversional method for the calculation of activation energy values in thermal reactions.

2.5. Syncrotron SAXS/WAXS study

SAXS/WAXS measurements were performed at the SAXS beamline [20] of the Laboratório Nacional de Luz Síncrotron (LNLS, Brazil). SAXS of the measurements were performed using a unidimensional detector at a wavelength of 1.608 Å (6.9 keV) and a sample-to-detector distance of 1143.2 mm. WAXS measurements were made simultaneously, using an image plaque detector in a cylindrical chamber.

3. Results and discussion

3.1. Flory–Huggins interaction parameter

The free energy of mixing ($\Delta G_m = \Delta H_m - T\Delta S_m$, where ΔH_m and ΔS_m are, respectively, the mixing enthalpy and entropy) should be negative in a miscible blend. For high molecular weight polymers, ΔS_m is negligibly small and ΔG_m sign is dominated by ΔH_m. Generally, ΔH_m is negative only if there are specific associative interactions between the two polymers [21].

In the present work, the dependence of T_m with T_c was studied applying the Hoffman–Weeks method [15] and the respective plot is shown in Fig. 1 for PEO and the different blend compositions. For blends PEO/PVPh-HEM with PVPh-HEM concentrations higher than 40 wt%, the T_m value cannot be observed. For this reason, the Hoffman–Weeks method was applied to blends with PVPh-HEM concentration up to 40 wt%. As shown in Fig. 1, the values of the equilibrium melting temperature, $T_{m,eq}$, can be evaluated by extrapolating linear least-squares fit lines of the experimental data according to Eq. (5) to intersect the line $T_m = T_c$ [15].

$$T_m = T_{m,eq}\left(1 - \frac{1}{\gamma}\right) + \frac{T_c}{\gamma} \tag{5}$$

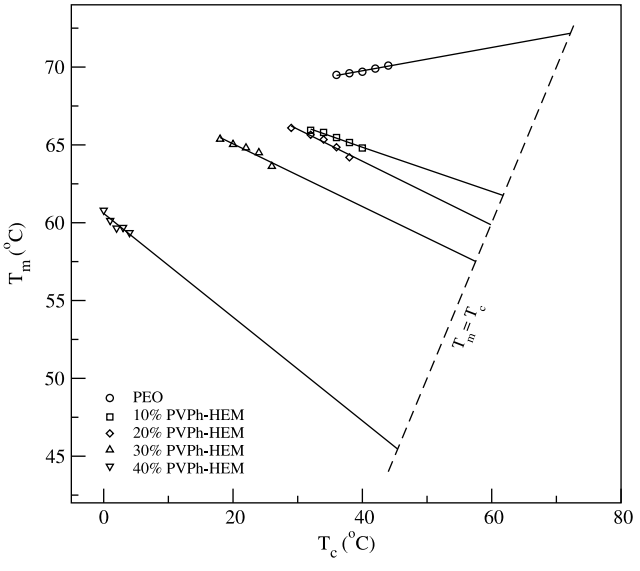

Fig. 1. Hoffman–Weeks plot for isothermally crystallised blends and for pure PEO.

where γ is the ratio of the lamellar thickness to the lamellar thickness of the critical nucleus at T_c. The equilibrium melting temperature determined in this way assumes that the crystals are perfect and of finite size and that no recrystallisation takes place during the melting run. In the last equation, the inverse of γ is allowed to assume values between 0 and 1 and is often called a stability parameter [12], which depends on the crystal thickness. According to this model, the higher values of γ indicate the most stable crystals, whereas inherently unstable ones should present lower values of γ. A non-linear behaviour on the T_m–T_c relation can lead to deviations on the $T_{m,eq}$ determination, which can be more pronounced in systems (homopolymers, copolymers or blends) in which the lamellar thickness does not change during the isothermal crystallisation. According to Weeks [22], the increase in T_m with T_c is merely a result of the increase in the lamellar thickness during the crystallisation, which simply indicates that more significant changes in the lamellar thickness are achieved at higher T_c values, as a result of the molecular mobility. In the present system, a small decrease in T_m with T_c can be observed, which is probably related to a crystallinity suppression effect or indicates that, during the isothermal crystallisation, there is no significant change on the thickness of the newly formed lamellae.

Fig. 2 shows the dependence of $T_{m,eq}$ on the PEO concentration. The melting point depression observed with PVPh-HEM concentration can be due to the decrease of the chemical potential of the crystallisable polymer caused by the addition of the miscible diluent. In addition, the crystals formed become less stable as PVPh-HEM is added to the blend. At a molecular level, hydrogen bonding interactions between PVPh-HEM and PEO take place, hindering the formation of crystalline PEO structures, as observed in a previous work [14].

The depression of $T_{m,eq}$ for a crystalline component in a polymer blend is used to determine the polymer–polymer interaction parameter, according to the equation derived by Nishi and Wang [23], which is based on the Flory–Huggins

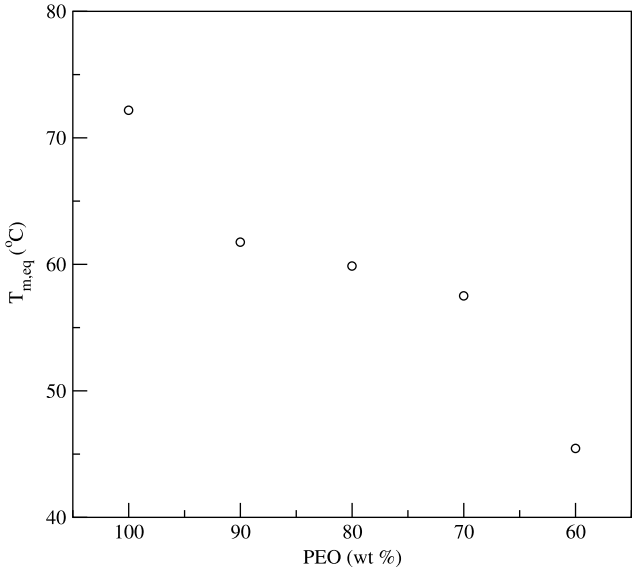

Fig. 2. $T_{m,eq}$ as a function of the PEO composition.

lattice theory [24]:

$$-\frac{\Delta H_{2u}V_{1u}}{RV_{2u}}\left(\frac{1}{T_{m,eq}}-\frac{1}{T^0_{m,eq}}\right)-\frac{\ln\phi_2}{m_2}-\left(\frac{1}{m_2}-\frac{1}{m_1}\right)\phi_1 = \beta = \chi_{12}\phi_1^2 \quad (6)$$

where $T^0_{m,eq}$ is the equilibrium melting temperature of the pure crystallisable component (in this case, PEO), ΔH_{2u} is the heat of fusion per mole of the repeating unit of PEO, V_iu the molar volume of the i component and R the ideal gas constant. A plot of β vs ϕ_1^2 should give a straight line passing through the origin if χ_{12} is assumed to be independent on the composition of the blend. In Fig. 3 the plots of β against ϕ_1^2 are shown for the compositions studied. The results showed in Fig. 3 were obtained from Eq. (6) using the parameters contained in Table 1.

For the blend PEO/PVPh-HEM, the points in Fig. 3 follow a logarithmic dependence, indicating a strong dependence of χ_{12} on the composition. In this case, χ_{12} is calculated for different blend compositions, obtained as the slope of the lines connecting each experimental point to the origin. The values calculated with this method are negative for all compositions studied. For a miscible blend formed of polymers of high m_i, χ_{12} must have a negative value, according to the Eq. (6). The variation of χ_{12} with the PEO composition on the blend is shown in Fig. 4.

Nishi and Wang [21] attribute the dependence of χ_{12} on the composition to morphological and kinetics factors, such as recrystallisation. However, Painter [25] proposed that this effect results from the strong interactions between the different components, such as hydrogen bonding, observed for this blend [14]. The negative values of χ_{12} clearly indicates that PEO and PVPh-HEM are miscible in the melt (due to strong intermolecular interactions), in the non-crystalline fraction of the solid and on the periphery of the crystals [26]. The miscibility between the components in the PEO/PVPh-HEM blend, as proved by the thermodynamic analysis, is a consequence of the specific interactions in the system and is an important feature for the application of this polymer matrix as host in solid electrolytes. The miscibility is also important in the formation of semi-crystalline nanostructures where PEO chains may keep part of the structural memory in a system where the overall crystallinity is lower than in the pure PEO.

Table 1
Parameters utilised in Eq. (6)

ΔH_{2u}	8.26 kJ mol^{-1}
R	8.31 kJ mol^{-1}
V_{PEO}	38.9 cm^3 mol^{-1}
$V_{PVPh\text{-}HEM}$	476.6 cm^3 mol^{-1}
m_{PEO}	9.1×10^4
$m_{PVPh\text{-}HEM}$	8.7×10^4

For application as a host matrix in a PSE, the polymeric system should exhibit a slow crystallisation kinetics, since the formation of crystalline phases may diminish the ion mobility in the solid. Each method and model for evaluation of the crystallisation kinetics allows a particular interpretation of the system. In the present work, the Avrami, Kissinger and Friedman methods were used to study the crystallisation kinetics of PEO/PVPh-HEM blends.

3.2. Isothermal crystallisation kinetics: Avrami method

The Avrami exponent obtained from the isothermal crystallisation reflects the mechanism of nucleation and growth of the crystals. Values of n about 1.0 indicate an homogeneous nucleation, usually in confined crystallisation process, while larger values, ranging from 2.0 to 4.0, suggest a breakout crystallisation, where crystals can grow in more than one-dimension.

In Table 2, crystallisation temperature (T_c), Avrami exponent (n), log(k) and crystallisation half time ($t_{1/2}$) for the different blend concentrations are shown as obtained for PEO

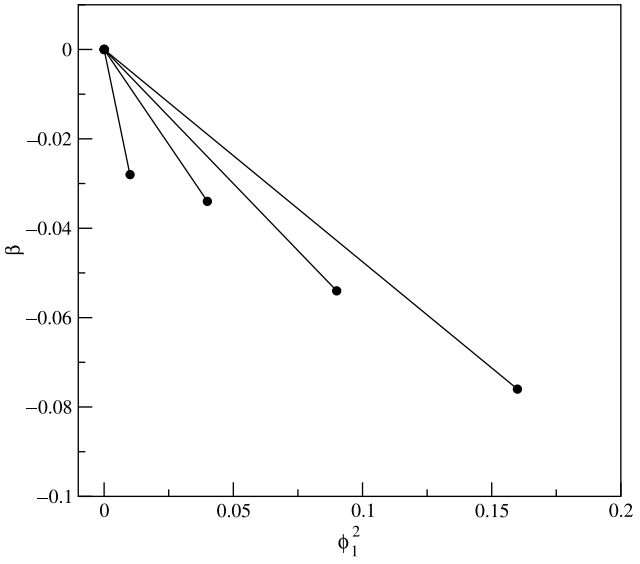

Fig. 3. Dependence of β on ϕ_1^2.

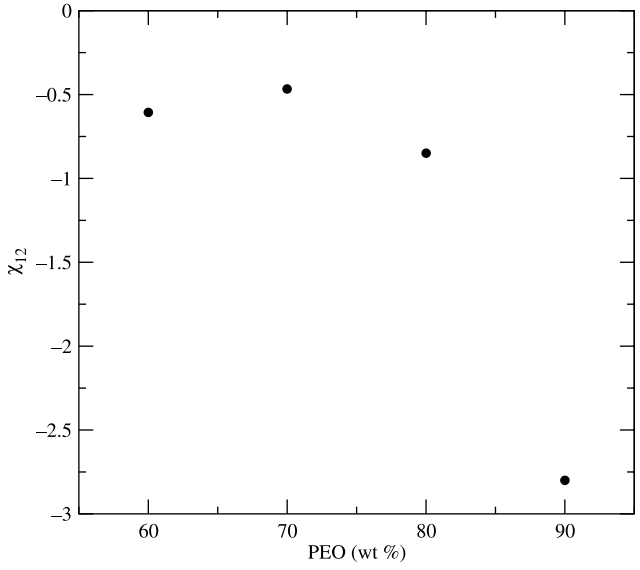

Fig. 4. χ_{12} as a function of PEO composition.

Table 2
Isothermal crystallisation kinetic parameters for different blends from the Avrami model

PEO (%)	T_c (°C)	Avrami exponent (n)	log(k)	$t_{1/2}$ (s)
100	25	4.49	−8.37	92
	28	3.9	−7.51	106
	34	3.97	−8.12	167
	38	3.92	−7.72	99
90	32	3.85	−7.38	109
	34	4.54	−9.18	147
	36	3.65	−7.12	141
	38	4.02	−8.16	158
	40	3.15	−6.50	148
80	30	3.48	−6.70	92
	32	2.98	−5.76	91
	34	3.10	−6.14	160
	36	3.00	−6.11	189
	38	2.75	−5.68	132
70	18	5.18	−10.47	123
	20	4.21	−8.53	126
	22	3.16	−6.31	145
	24	3.00	−6.67	190
	26	3.24	−6.64	129
60	0	3.23	−6.09	132
	1	3.40	−6.18	103
	2	6.42	−12.70	100
	3	5.02	−10.45	144
	4	4.82	−9.73	110

and the blends containing 10 up to 40% PVPh-HEM. The Avrami exponent is practically independent on the temperature over the temperature range studied for each blend composition. For pure PEO, the value of n is between 3.92 and 4.49. This values higher than 3 are associated to process of instantaneous nucleated three dimensional growth or sporadic nucleated two-dimensional growth.

From data listed in Table 2 it is clearly seen the increase in $t_{1/2}$ values as a consequence of PVPh-HEM incorporation. This indicates that the crystallisation rate of PEO decreases with the concentration of PVPh-HEM concentration. The slow-down of the crystallisation may arise from a physical restriction to the crystal growth, induced by the specific interactions between PEO and PVPh-HEM. Conclusively, the presence of PVPh-HEM does not change significantly the mechanism of crystallisation of PEO, but reduces the crystallisation rate of PEO in the blends compared to pure PEO.

3.3. Non-isothermal crystallization kinetics

Fig. 5 shows DSC curves at different cooling rates for PEO and blends containing from 10 up to 40% PVPh-HEM, during the crystallisation process. A positive shift in the peak temperature for increasing cooling rates can be clearly observed, due to the fact that samples are closer to thermal equilibrium at lower cooling rates. The shape of the curves indicates one single crystallisation process, attributed to the crystallisation of a miscible PEO-rich phase from the melt. The peak temperature is shifted to lower values as the amount of PVPh-HEM increases in the blend, as observed from DSC curves at the same cooling rate for different samples, which indicates that the crystallisation of the blends is slower then the pure PEO and the increase in PVPh-HEM concentration inhibits PEO crystallisation.

3.3.1. Kissinger method

The Kissinger method was initially developed for first-order reactions but, in fact, it holds for any kinetic model [17]. This method assumes that the reaction rate is maximum at the peak of the DSC curve and the reaction order remains constant during the process. Thus, plotting the natural logarithm of the heating rate (θ) divided by the square of the absolute peak temperature (T_p^2) vs the inverse of the peak temperature, a straight line should be obtained, which slope is directly related to the apparent activation energy (E_a).

Plots of $\ln(\theta/T_p^2)$ vs $-1/T_p$ are shown in Fig. 6. For all the samples the analysis fitted a straight line with a good correlation, from which E_a values were obtained. It can be seen, from the values listed in Table 3, that the addition of PVPh-HEM to PEO diminishes the apparent activation energy for the crystallisation process, despite the fact that incorporation of PVPh-HEM in PEO causes a decrease in the size of the crystallites, as observed by polarised light optical microscopy in a previous work [15]. This phenomenon takes place probably due to the nucleation process of the PEO chains, for which the increase in PVPh-HEM concentration promotes the formation of a larger number of nucleation centres. Apparently, these already nucleated centres have their growth process inhibited by the specific interactions between PEO and PVPh-HEM, up to 50/50% mass ratio and for PVPh-HEM concentrations higher than 50%, the melting peak of the crystalline phase is not observed, indicating the suppression of the blend crystallinity.

The comparison between two different kinetic models allows a more clear interpretation of the experimental results. However, methods based on different assumptions should obviously present different (however, consistent and convergent) results. In the present work, results on the crystallisation kinetics based on the Kissinger and Friedman methods are compared for a more clear description of the activation energy for the crystallisation of PEO/PVPh-HEM blends.

3.3.2. Friedman method

Assuming that crystallisation is a single-step reaction and that the rate constant obeys the Arrhenius law, Friedman proposed an isoconversional method for kinetic studies, which allows the determination of the different activation energies for each degree of conversion directly from DSC data, without a knowledge of the conversion function [27]. In the present work, Friedman analysis was conducted considering $\alpha = 0.5$, which is near to the maximum of the peak temperature and equivalent to the Kissinger analysis for comparison.

Friedman analysis was carried out plotting $\ln(dH/dt)$ vs $-1/T$, as shown in Fig. 7 and the values of $E_{0.5}$ are listed in Table 3. The effective energy barrier governing the crystallisation process of the PEO/PVPh-HEM blends was found to decrease as the concentration of PVPh-HEM increases.

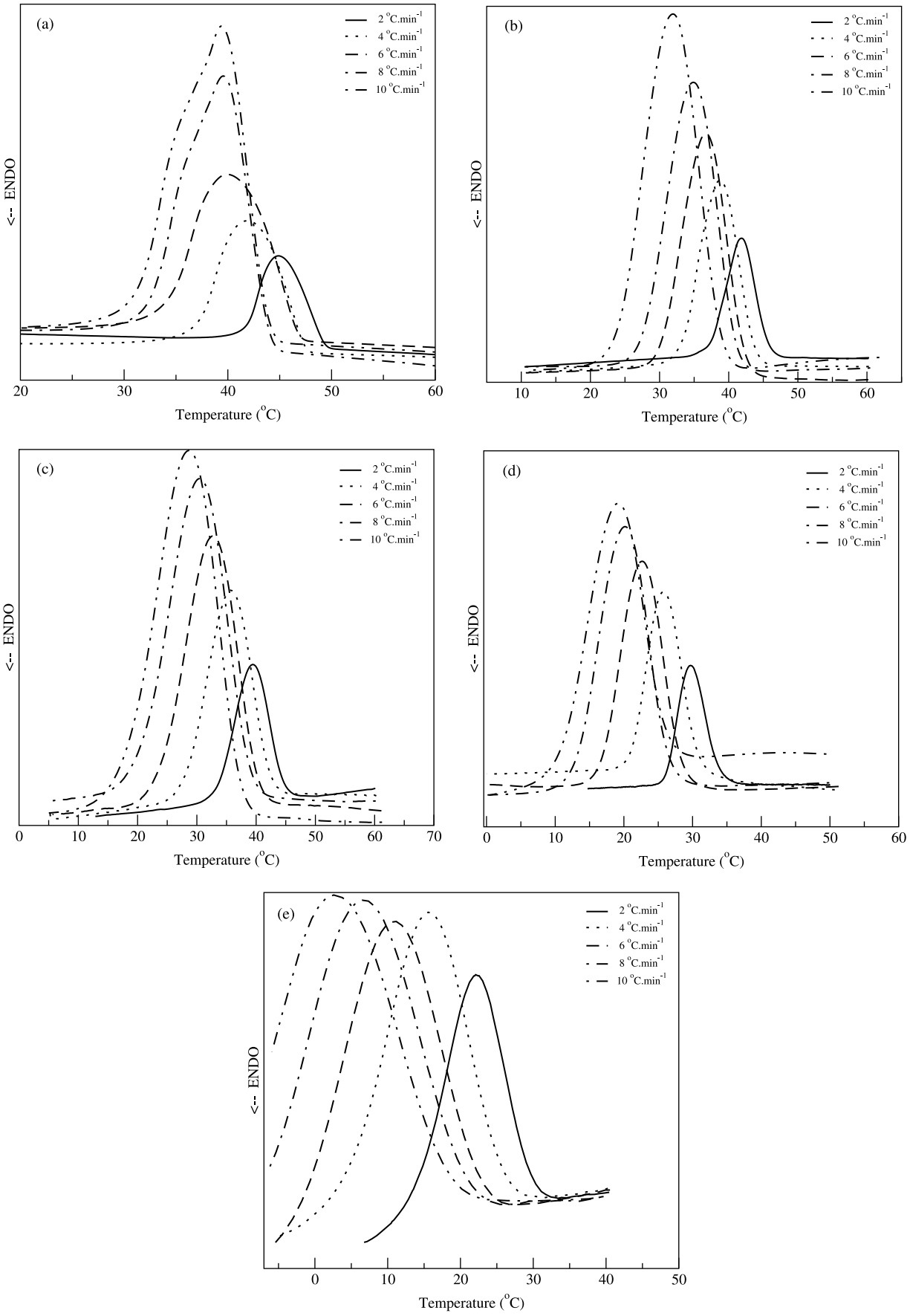

Fig. 5. DSC curves for non-isothermal crystallisation of PEO (a) and the blends containing (b) 10%; (c) 20%; (d) 30%; and (e) 40% of PVPh-HEM.

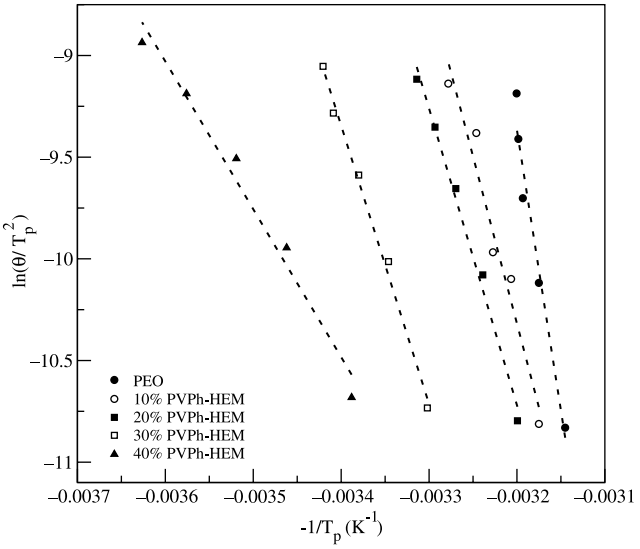

Fig. 6. Kissinger plot for crystallisation of PEO and the blends.

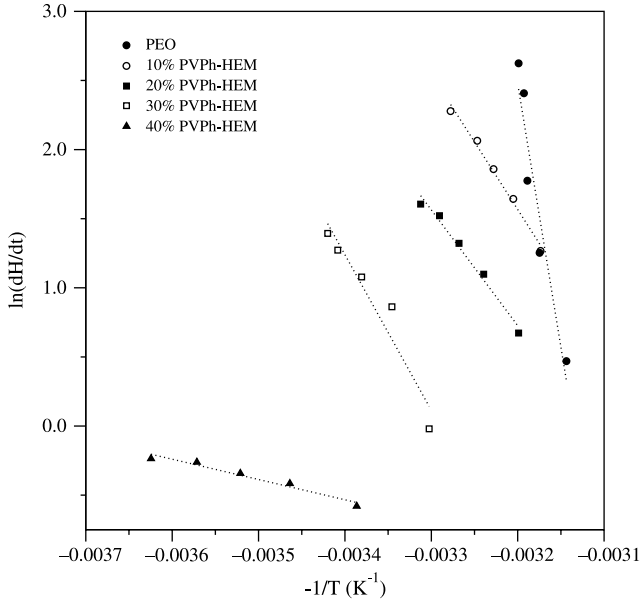

Fig. 7. Friedman analysis for crystallisation of PEO and PEO/PVPh-HEM blends.

Similarly to the observed with the Kissinger method, the decrease in the $E_{0.5}$ values may be due to the most favourable environment for the nucleation process, while the crystal growth is inhibited by the interactions between PEO and PVPh-HEM.

From the values exhibited in Table 3, it can be seen that the effective energy barrier for the crystallisation decreases for increasing concentration of the miscible component, PVPh-HEM. In this system, hydrogen bond interactions take place between PVPh-HEM and PEO in the solid state, which are responsible for the miscibility of the system and, probably, also for the changes in the apparent activation energy of crystallisation for the blends, as calculated utilising both Kissinger and Friedman methods. The two methods for calculating activation energy presented different but convergent values and these differences can be attributed to the initial assumptions of each one. The choice of a method for calculating kinetic parameters from DSC curves must be oriented to the kind of system under investigation and to the parameters to be studied, and, combining the analysis of the Kissinger and Friedman methods, a decrease in the energy barrier for the crystallisation process of PEO/PVPh-HEM blends is observed, in comparison to pure PEO, despite the slower kinetics of this process, evidenced by the lower $t_{1/2}$ values for the blend (in comparison to pure PEO), obtained from the Avrami analysis to the isothermal crystallisation experiments.

In pure PEO crystallisation, due to the high system viscosity, in the melt (which inhibits the diffusivity of the PEO chains towards the crystal nuclei), the energy barrier for the crystallisation process depends on the chain diffusion, as well as on the formation of the nucleation centres. In the crystal growth regime, a competition among the newly crystallised centres takes place. In PEO/PVPh-HEM blends, the diffusion of PEO chains for the crystal formation may be favoured in the melt and in the miscible, non-crystalline PEO/PVPh-HEM phase around the newly nucleated centres may generate a confinement effect, avoiding the competition among these centres in the crystal growth regime. As a consequence of this behaviour, a decrease in the energy barrier for the crystallisation process is observed in PEO/PVPh-HEM blends, comparatively to the pure PEO.

Table 3
Apparent activation energy from the non-isothermal crystallisation kinetics for different blends from the Kissinger (E_a) and Friedman ($E_{0.5}$) models

PEO/PVPh-HEM	E_a (kJ mol^{-1})	$E_{0.5}$ (kJ mol^{-1})
100/0	229.1	317.0
90/10	136.8	93.6
80/20	121.3	81.4
70/30	113.7	69.6
60/40	60.4	12.2

3.4. Synchrotron SAXS/WAXS measurements

The nanostructure of the host matrix is decisive to the transport properties of solid electrolytes, especially, in PSE which the transport mechanism is governed by the migration of ions from one coordinating site to a next one. Bruce and Andreev [7] studied PEO/Li^+ electrolytes and suggested that the helical structure of PEO should be maintained (however, distorted) in order to enhance the unidimensional conductivity (Li^+ inside the helical PEO chain) and, consequently, the overall conductivity of the PSE. In the present work, synchrotron SAXS/WAXS profiles were obtained for PEO/PVPh-HEM blends is order to study the semi-crystalline nanostructure of the material and its dependence with the blend composition.

Lorentz-corrected SAXS profiles for PEO/PVPh-HEM blends and of pure PEO and PVPh-HEM are shown in Fig. 8. The scattering intensity decreases with increasing concentration of PVPh-HEM, due to decreasing electron density contrast ($\Delta\eta = \eta_c - \eta_a$) between the crystalline and non-crystalline layers. The electron density of the interlamelar regions is

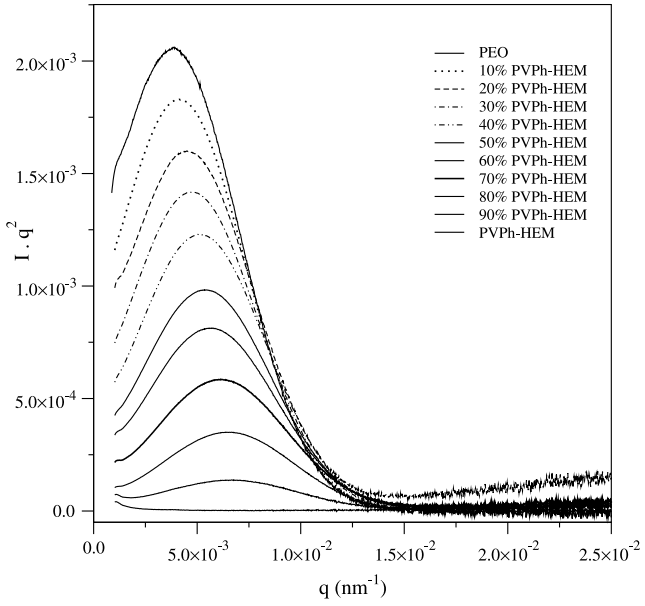

Fig. 8. Lorentz corrected SAXS patterns of PEO/PVPh-HEM blends at ambient temperature.

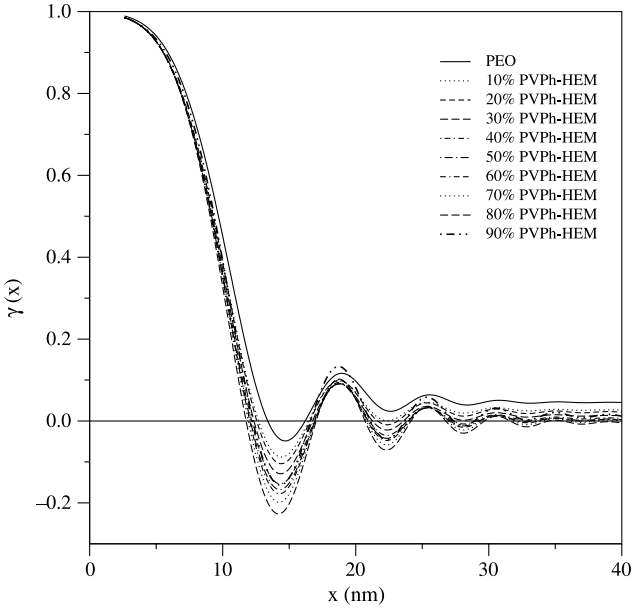

Fig. 9. Linear correlation functions of PEO and PEO/PVPh-HEM blends at ambient temperature.

probably increased due to incorporation of PVPh-HEM into it, as this would decrease the electron density contrast between the crystalline and non-crystalline layers, similarly to the observed in the work of Chen and Wang [28]. A second-order peak can not be clearly identified, indicating a fairly well lamellar stacking in the samples.

The long period (L_p) associated with the lamellar stacks can be calculated from the peak maximum of the Lorentz-corrected SAXS profiles using the Bragg's equation ($L_p = 2\pi/q_{max}$) or by the one-dimensional correlation function, $\gamma(x)$; the method chosen in the present work. The correlation function, defined by Strobl and Schneider, adopts the following form [29]:

$$\gamma(x) = \frac{\int_0^\infty I(q)q^2 \cos(2\pi \times q)\mathrm{d}q}{\int_0^\infty I(q)q^2\mathrm{d}q} \quad (7)$$

where $I(q)$ is the absolute scattering intensity obtained from the SAXS measurement, q is the scattering vector, and x is the direction along which the electron density is measured. Since the experimentally accessible q range is finite, extrapolation of intensity to both low and high q is necessary for the integrations. Extrapolation to zero q was accomplished by the Debye–Bueche model [30,31] and for large q values was performed using the Porod–Ruland model [32].

In Fig. 9, the plots of correlation function for the different PEO/PVPh-HEM blends and the pure PEO are shown, from which the invariant (Q_0), long period (L_p), crystalline (R_c) and non-crystalline (R_n) layer thickness, listed in Table 4, were obtained [33]. L_p values for PEO and the blends exhibit a roughly constant value at near 9.9 nm with an insignificant composition dependence. In the lamellar stack model with sharp phase boundary, the long period represents the sum of R_c and R_n. Two approaches may be utilized to determine the average thickness of these two layers, namely, the one-dimensional correlation function and the interphase distribution function. The one-dimensional correlation function was utilized to deconvolute L_p into the thickness of these two layers.

From Table 4, the dependence of R_c and R_n on the PVPh-HEM concentration in PEO/PVPh-HEM blends are shown and, like the long period, R_c and R_a do not present significant variation with PVPh-HEM concentration. This weak dependence of the structural parameters on the PVPh-HEM concentration can be associated with the assumption of the two phase (crystalline/non-crystalline) model, where the thickness of the non-crystalline/crystalline interphase (R_i) is included into the values of R_c and R_n [32]. The interphase thickness for the blend samples appears to be <1 nm, which is much smaller than R_c or R_n. These small R_i values may be responsible for the observed weak functions of PVPh-HEM for R_c, while the weak dependence of R_n on PVPh-HEM concentration indicates the formation of an extralamellar morphology, without significant change in the interlamellar

Table 4
Structural parameters obtained from the SAXS profiles for PEO/PVPh-HEM blends

PEO (%)	Q_0 ($\times 10^{-6}$)	L_p (nm)	R_c (nm)	R_n (nm)
100	13.65	9.9	8.3	4.6
90	12.07	9.8	8.1	3.9
80	10.85	9.8	8.1	3.8
70	9.33	9.7	8.1	4.1
60	8.12	9.7	8.0	4.0
50	6.55	9.6	8.0	4.0
40	5.39	9.6	8.0	4.3
30	3.89	9.6	8.1	4.2
20	2.29	9.5	8.1	4.3
10	0.96	9.5	8.2	4.5
0	0.047	–	–	–

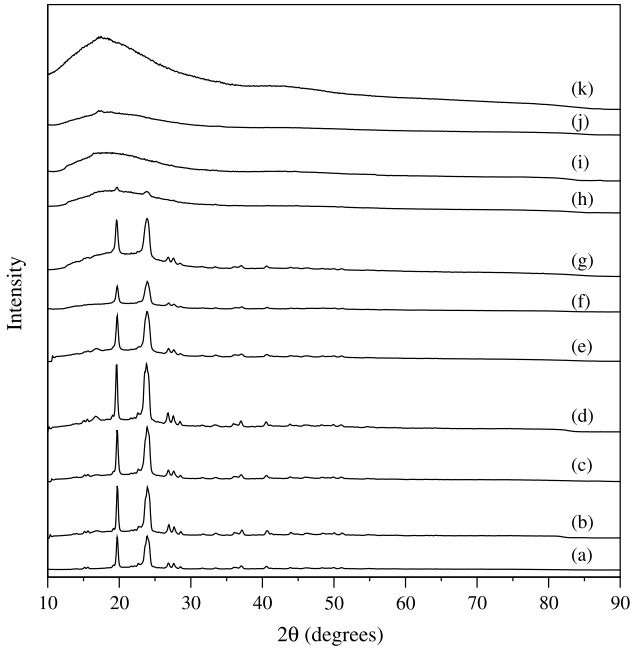

Fig. 10. WAXS patterns of PEO/PVPh-HEM blends at ambient temperature. (a) PEO; (k) PVPh-HEM; blends containing: (b) 10%; (c) 20%; (d) 30%; (e) 40%; (f) 50%; (g) 60% (h) 70%; (i) 80%; (j) 90% PVPh-HEM.

regions. This extralamellar highly disordered morphology is probably formed due to the high molecular mass of the PEO used in the present work and to the incorporation of a non-crystalline diluent which affects the crystal growth rate, as discussed previously in the present work.

Fig. 10 shows the WAXS profiles of PEO/PVPh-HEM blends compared to those of pure PEO and PVPh-HEM. It is seen that the PVPh-HEM does not exhibit crystalline peaks, while the WAXS profile of PEO presents the two characteristic crystalline peaks at 19.78 and 23.98° [34]. These peaks are clearly seen for blends containing 10–60 wt% PVPh-HEM but are found to be absent in the blends containing more than 70 wt% PVPh-HEM. Additionally, the area of the non-crystalline halo increases in the WAXS profiles of these blends. As observed in a previous paper [15], the crystallinity of PEO/PVPh-HEM blends is highly dependent on the inter- and intramolecular specific interactions, such as hydrogen bonding, which is responsible for the miscibility and also the suppression of the crystallinity of the system.

According to Rajendran and co-workers [35], a fully non-crystalline morphology produces greater polymer flow and ionic diffusivity in PEO-based polymer electrolytes, in which high ionic conductivity can be obtained in non-crystalline polymers having highly flexible backbones and low glass transition temperatures. However, Andreev and Bruce [7,36,37] showed that some degree of organization in the non-crystalline phase is required for achieving higher conductivities. The chain organization in the non-crystalline phase observed in the present work for blends with PVPh-HEM concentrations above 70 wt% can be considered as a crystalline structural memory of PEO chains, which is directly controlled by the inter- and intramolecular interactions and defines the nanostructure of the solid.

The values of R_c and R_n, virtually independent on the PVPh-HEM concentration, indicate that the PEO lamellae exist even at high concentrations of PVPh-HEM, despite the suppression of the crystallinity, as evidenced by WAXS measurements. For PVPh-HEM concentrations higher than 70%, WAXS profiles show only the presence of a non-crystalline halo, while the R_c values indicate that the PEO lamellae keep approximately the same thickness than in pure PEO. Considering that PEO lamellae are originated from the organisation of its helical chains arrangement [38], it can be inferred that, for the non-crystalline blends with high concentrations of PVPh-HEM, PEO chains keep their crystalline structural memory. This structural characteristic is the connection (at a molecular level) between the nanostructure and the ionic conductivity in solid electrolytes PEO/LiX, as suggested by Andreev and Bruce [36,37], where the proposed model for Li^+ conduction involves the ion displacement inside the PEO helical chains. Significant structural changes are expected when Li^+ is complexed by PEO chains, however, the structure of the PEO/PVPh-HEM blend is promising considering the maintenance of the crystalline structural memory in a non-crystalline system.

4. Conclusions

PEO/PVPh-HEM blends obtained by casting from solvent are miscible, from the observation of the negative values for the Flory-Huggins interaction parameter. The dependence of χ_{12} with composition is associated to the strong hydrogen bonds that take place between the polymers and the decrease observed in its experimental values corresponds to a prevalence of intermolecular rather than intermolecular interactions in the blends. These specific interactions respond for both thermodynamic and kinetic (related to crystallisation) aspects. Suppression of the crystallinity and decrease of the activation energy for the crystallisation of the blends are direct consequences of the miscibility of the system.

The isothermal crystallisation kinetic study with the Avrami model showed that the presence of PVPh-HEM does not change significantly the mechanism of crystallisation of PEO, but reduces the crystallisation rate of PEO in the blends compared to pure PEO, as observed in $t_{1/2}$ values of the blends in comparison to the pure PEO sample. From the Kissinger and Friedman analysis of the non-isothermal crystallisation kinetics, it was shown that the addition of PVPh-HEM to PEO diminishes the apparent activation energy for the crystallisation process. Despite the lower activation energy, caused by a more favourable structure where part of the PEO chains are probably excluded from a miscible PEO/PVPh-HEM phase, the crystallisation time is reduced in the blends comparatively to the pure PEO, due to time needed for the diffusion of PEO chains from the miscible melt to the crystal centres.

From the SAXS/WAXS studies, the weak dependence of the structural parameters R_c and R_n on the PVPh-HEM

concentration was evidenced and is associated with the interphase thickness, which is much smaller than R_c or R_n, indicating the formation of an extralamellar morphology. For the non-crystalline blends with high concentrations of PVPh-HEM, PEO chains probably keep their crystalline structural memory. This structural characteristic is the connection (at a molecular level) between the nanostructure and the ionic conductivity in solid electrolytes PEO/LiX.

Acknowledgements

Authors would like to thank the Brazilian National Research Council (CNPq) for fellowships, FAPERJ (Process n°. E-26/170.700/2004) for support of this work, and the Laboratório Nacional de Luz Síncrotron (LNLS) in Brazil for support and assistance with the synchrotron SAXS measurements.

References

[1] Pereira RP, Rocco AM, Bielschowsky CE. J Phys Chem B 2004;108:12677.
[2] Acosta JL, Morales E. J Appl Polym Sci 1996;60:1185.
[3] Mastragostino M, Arbizzani C, Meneghello L, Paraventi R. Adv Mater 1996;8:331.
[4] De Paoli M-A, Zanelli A, Mastragostino M, Rocco AM. J Electroanal Chem 1997;435:217.
[5] Bruce PG, editor. Solid state electrochemistry. Cambridge: Cambridge University Press; 1997. p. 106.
[6] Armand MB. In: McCallum JR, Vincent CA, editors. Polymer electrolyte reviews. London: Elsevier Applied Science; 1989. p. 1.
[7] Andreev YG, Bruce PG. Eletrochim Acta 2000;45:1417.
[8] Rocco AM, Pereira RP, Felisberti MI. Polymer 2001;42:5199.
[9] Rocco AM, Fonseca CP, Pereira RP. Polymer 2002;43:3601.
[10] Zhu L, Mimnaugh BR, Ge Q, Quirk RP, Cheng SZD, Thomas EL, et al. Polymer 2001;42:9121.
[11] Bodycomb J, Yamaguchi D, Hashimoto D. Macromolecules 2000;33:5187.
[12] Cohen LE, Rocco AM. J Therm Anal Calorim 2000;59:625.
[13] Guo Q, Harrats C, Groeninckx G, Koch MHJ. Polymer 2001;42:4127.
[14] Guo Q, Harrats C, Groeninckx G, Reynaers H, Koch MHJ. Polymer 2001;42:6031.
[15] Rocco AM, Bielschowsky CE, Pereira RP. Polymer 2003;44:361.
[16] Hoffman JD, Weeks JJ. J Res NBS Phys Chem 1962;66:13.
[17] Avrami M. J Chem Phys 1939;7:1103. Avrami M. J Chem Phys 1940;8:212. Avrami M. J Chem Phys 1941;9:177.
[18] Kissinger HE. Anal Chem 1957;29:1702.
[19] Friedman HL. J Polym Sci, Part C: Polym Symp 1964;6:183.
[20] Kellermann G, Vicentin F, Tamura E, Rocha M, Tolentino H, Barbosa AJ, et al. J Appl Crystallogr 1997;30:880.
[21] Billmeyer FW. Textbook of polymer science. New York: Wiley; 1984.
[22] Weeks JJ. J Res Natl Bur Stand A 1963;67:441.
[23] Nishi T, Wang TT. Macromolecules 1975;8:909.
[24] Flory PJ. Principles of polymer chemistry. New York: Cornell University Press; 1953 [chapters 12, 13].
[25] Painter PC, Shenoy SL, Bhagwagar DE, Fisburn J, Coleman MM. Macromolecules 1991;24:5623.
[26] Xing P, Dong L, An Y, Feng Z, Avella M, Martuscelli E. Macromolecules 1997;30:2726.
[27] Sbirrazuoli N, Girault Y, Elegant L. Thermochim Acta 1997;293:25.
[28] Chen HL, Wang SF. Polymer 2000;41:5157.
[29] Strobl GR, Schneider MJ. Polym Sci, Polym Phys Ed 1980;18:1343.
[30] Debye P, Bueche AM. J Appl Phys 1949;20:518.
[31] Debye P, Anderson Jr HR, Brumberger HJ. J Appl Phys 1957;28:679.
[32] Ruland WJ. J Appl Crystallogr 1971;4:70.
[33] Triolo A, Visalli G, Triolo R. Solid State Ionics 2000;133:99.
[34] Tadokoro H. Macromolecules 1984;25:147.
[35] Rajendran S, Mahalingam T, Kannan R. Solid State Ionics 2000;130:143.
[36] MacGlashan GS, Andreev YG, Bruce PG. Nature 1999;398:792.
[37] Gadjourova Z, Andreev YG, Tunstall DP, Bruce PG. Nature 2001;412:520.
[38] Takahashi Y, Tadokoro H. Macromolecules 1973;6:672.